

Modeling confinement in polymer nanocomposites from linear viscoelasticity data

Xun Chen¹ · Margaret J. Sobkowicz¹

Received: 29 December 2014 / Revised: 3 July 2015 / Accepted: 24 August 2015 / Published online: 5 September 2015
© Springer-Verlag Berlin Heidelberg 2015

Abstract The ability of the time-dependent diffusion–double-reptation (TDD-DR) theory to predict the molecular structure and dynamics of polymer nanocomposites is investigated for poly(butylene succinate) blended with fumed silica particles with contrasting surface treatments (unmodified and modified with silanes). Structural and dynamic parameters such as confined polymer fraction (ϕ_s) and relaxation time are extracted from fitting the experimental curves for relaxation modulus $G(t)$ by the TDD-DR model with fluctuation effects included. A good fit of experimental data over seven time decades is obtained after modification of the TDD-DR model to account for Rouse relaxation on the short time scale. The fraction of confined polymer extracted from model fitting is in quantitative agreement with the value obtained from the specific reversing heat capacity for poly(butylene succinate) (PBS)/fumed silica nanocomposites. Based on parameters deduced from rheological data, we study the influence of surface functionality on the microstructure of polymer matrix. We conclude that increasing the polymer–particle compatibility through introduction of a hydrophobic functionality on the surface of the particles results in increased amount of confined PBS chains and strong immobilization of the PBS molecules. These interface effects are discussed for the first time in terms of TDD-DR model that takes into account the dynamics of bound polymer chains, allowing prediction of the universal

nature of the confinement effect and its role in polymer nanocomposite processing and bulk physical properties.

Keywords Reptation · Linear viscoelasticity · Stress relaxation

Introduction

Polymer composites with nanoscale fillers have received great attention due to their enhanced thermophysical properties and potential high performance (Chou 1993; Leblanc 2009). Current research (Kabanemi and Héту 2013; Oh and Green 2008) has shown that the property improvements in nanocomposites are mainly related to the dispersion state and the dynamics of the polymer chains, both of which are affected by the surface functionality of the fillers. Over the past decades, several theoretical models have been proposed to explain this filler-induced reinforcement. Long and Sotta (2007) suggested that mechanical reinforcement occurs when the confined glassy regions surrounding the nanoparticles overlap, forming a percolating structure. Another theory to explain the reinforcement mechanism is the “bridge effect” (Zhu and Sternstein 2003; Zhu et al. 2005). For nanoparticles such as carbon nanotubes (CNTs) as well as silica, mechanical reinforcement appears to depend on a strong surface–polymer interaction that physically bonds the chains to the filler surface and results in a “bridging effect” (Aranguren et al. 1992; Jouault et al. 2009), manifested in a higher entanglement density than for the neat polymer (Anderson and Zukoski 2009; Sarvestani and Picu 2004, 2005). From rheological and small-angle scattering analysis, Kumar et al. suggested that reinforcement can be maximized by the formation of a temporary but long-lived polymer–particle network with the particles serving as the network junctions (Akcora et al. 2009a, b,

Electronic supplementary material The online version of this article (doi:10.1007/s00397-015-0872-9) contains supplementary material, which is available to authorized users.

✉ Margaret J. Sobkowicz
Margaret_SobkowiczKline@uml.edu

¹ Plastics Engineering Department, University of Massachusetts Lowell, One University Avenue, Lowell, MA 01854, USA

2010; Harton et al. 2010; Moll et al. 2011). Our previous work also demonstrated that persistence of polymer–filler temporary networks is controlled by the particle surface chemistry: with organically modified particles incorporated in the polymer matrix, polymer chain confinement caused by stronger polymer–particle interactions leads to the suppression of the terminal zone which is replaced by a rubbery behavior (Chen et al. 2014). The aim of the present work is to quantify the filler confinement effect for contrasting surface functionalities in molten polymer nanocomposites from viscoelasticity data.

In general, the viscoelastic properties of polymer nanocomposites depend on structural factors, such as the volume fraction, size and shape of filler particles, and on interactions among the components. It is well known that the polymer–filler interactions are dominant, and this interaction should be considered frictional in nature (Anderson and Zukoski 2009; Dionne et al. 2005; Havet and Isayev 2001, 2003; Sarvestani and Picu 2005; Simhambhatla and Leonov 1995; Subbotin et al. 1997). Numerous models have been proposed to describe the rheological behavior of nanofilled polymers with this dominant polymer–filler interaction (Sarvestani 2008; Sarvestani and Jabbari 2006, 2008; Sarvestani and Picu 2004; Sarvestani and Picu 2005; Simhambhatla and Leonov 1995). The transition from liquid-like to solid-like behavior at low frequency in dynamic mechanical spectroscopy has been attributed to a lag in relaxation of chains strongly interacting with the fillers. Other approaches model the rheology of polymer nanocomposites using the classic polymer-reptation theories (de Gennes 1971; Doi and Edwards 1978, 1986; Havet and Isayev 2001, 2003). Unlike other constitutive or phenomenological models, the reptation theory and its extended models relate the rheology to the molecular structure and chain mobility. A reptation-based model that incorporates polymer–particle interactions and confinement was developed by Kabanemi and Héту (2010, 2013) to describe the dynamics and rheological behavior of linear entangled polymers filled with isotropic nanoscale particles. Kabanemi’s model predicted that liquid-like behavior is only exhibited after long times or low shear rates for high particle volume fraction, in good agreement with experimental observation (Zhang and Archer 2002). Sarvestani (2008) described two time regimes represented by reptation of “trapped” and “free” chains as Sternstein and Zhu (2002) proposed. This work utilized a two-phase model combined with Doi–Edwards reptation theory to model the solid-like response at low-frequency regimes for entangled polymer nanocomposites with strong polymer–filler interactions. The Sarvestani model correctly captured the solid-like behavior at low-frequency regimes, but failed to match with the data at high frequency regimes because of the neglected fluctuation and Rouse relaxation mechanisms.

The critical structure information such as fraction of adsorbed chains was also determined by curve fitting to the experimental data.

Chain confinement has also been examined using other techniques such as NMR relaxation measurements (Litvinov and Spiess 1991; Litvinov and Zhdanov 1987), dielectric spectroscopy (Kirst et al. 1993), dynamic mechanical thermal analysis (DMTA) (Mortezaei et al. 2011; Tsagaropoulos and Eisenberg 1995), and neutron scattering studies (Arrighi et al. 1998; Gagliardi et al. 2001). By means of advanced thermal analysis methods, Sargsyan et al. (2007) and Chen et al. (2009) and Ma et al. (2011) introduced the concept of “rigid amorphous fraction (RAF)” to describe such an immobilized layer, where the nanoparticles behave as an attractive surface that stiffens the polymer in close proximity. As defined in the RAF theory, the confined layer relaxes before the fulfillment of melting at T_m , disappearing in the same temperature range or before the crystal melting (Ma et al. 2011). Thus, the RAF theory only describes confinement in solids. The universal nature of the confinement effect and its role in nanocomposite bulk physical properties and processability remain unknown. Important questions to be answered are do the confined dynamics still exist in the melt state? What is its effect on the chain dynamics and properties of molten polymers? Since the addition of fillers dramatically changes the viscoelastic response of polymers, melt rheology is a good tool to address these questions (Drozdov et al. 2009; Liu et al. 2012; Mortezaei et al. 2011; Najafi et al. 2012; Shenoy 1999).

In this paper, we study the molecular structure and dynamics in poly(butylene succinate) (PBS)/fumed silica nanocomposites from knowledge of linear viscoelastic response. Our previous research revealed that polymer–filler surface interactions play an essential and dominant role in the segmental dynamics of PBS/fumed silica nanocomposites, so we do not consider the particle–particle interaction to be within the experimental timescale in the present study (Chen et al. 2014). Building on previous models, we utilize the double-reptation (des Cloizeaux 1988; Tsenoglou 1987, 1991) and time-dependent relaxation (des Cloizeaux 1990) theories, which cover the reptation behavior, Rouse processes, and fluctuation effects. This allows us to obtain information on molecular structure and dynamics from viscoelastic data and to reproduce the linear viscoelastic response of polymer nanocomposites. Based on the modeling results, we can solve the “inverse question” to find the dependence of bound polymer fraction on surface treatment of fillers without considering the primary size and shape of the fillers. The amount of the immobilized polymer layer calculated from the model is also compared with the RAF obtained from the specific reversing heat capacity.

Theoretical background

Model

In the present work, the polymer matrix is assumed to be partitioned into two fractions with different chain dynamics: one confined by the fillers and the other the unconfined fraction. This partitioning follows from not only Sarvestani (2008) but independently from Gagliardi et al. (2001), who studied the quasi-elastic neutron scattering (QENS) spectra of polymer–filler systems and confirmed the existence of two dynamic processes of polymer matrix: a quasi-elastic component due to chains not affected by the presence of fillers and an elastic component from chains whose dynamics are strongly restricted. The unconfined polymer chains simply diffuse with unperturbed reptative motion, whereas the confined polymer can only diffuse away from the surface after longer-term strain loading. It should be noted that this binary model does not distinguish between different degrees of surface interaction that might result in variation in the strength of immobilization (Harton et al. 2010). However, because the goal was to characterize the strength of interactions for distinct surface functionalities, in the current research, the two-phase model was deemed sufficient. Thus, we assume that the bound layers examined herein should display the same degree of tightness for the same filler. Sarvestani assumed that the diffusion of adsorbed chains can be considered to be somewhat similar to the process of sticky reptation of associating polymers (Sarvestani 2008). Hence, the relaxation mechanism in the current system, where polymer chains display both fast and slow relaxation dynamics, seems to be close to the double-reptation concept which has been widely applied for binary polymer blends. In the following section, the formulation for the double-reptation theory to describe and capture rheology features of PBS/fumed silica nanocomposites is described.

According to double-reptation theory, the relaxation modulus $G(t)$ can be written as

$$G(t) = G_N \left(\sum \phi_a \cdot F_a(t) \right)^\beta \quad (1)$$

Here, G_N is the plateau modulus, $F(t)$ is the relaxation function of each fraction, β is an index that characterized the mixing behavior. If $\beta = 1$, it means the polymer chains from each fraction relax independently, following a classic-reptation model. When $\beta = 2$, the relaxation of polymer chains will be affected by the diffusion of surrounding chains, following the double-reptation model proposed by Tsenoglou (1987). Instead of presuming that the molecules relax independently, the double-reptation theory takes account into the topological interaction between a pair of chains. In the case of molten polymers filled with nanofillers, the interaction between the chains attached on the particle surface and the polymers far away from the filler should not be neglected.

According to the time-dependent diffusion (TDD) model developed by des Cloizeaux (1990), the relaxation function $F(t)$ can be expressed as

$$F(t) = \frac{8}{\pi^2} \sum_{p \text{ odd}} \frac{1}{p^2} \exp(-p^2 U(t)) \quad (2)$$

$$U(t) = \frac{t}{\tau_{\text{rep}}} + \frac{1}{H} g\left(\frac{Ht}{\tau_{\text{rep}}}\right) \quad (3)$$

$$g(y) = -y + y^{0.5} \left[y + (\pi y)^{0.5} + \pi \right]^{0.5} \quad (4)$$

$$H = \frac{M}{M^*} \quad (5)$$

where τ_{rep} is the reptation time of polymer. The distribution function $U(t)$ consists of two terms: the first represents relaxation by reptation and the second specifically represents contributions of fluctuations. The weight of the fluctuation term depends on the value of a new material parameter M^* . des Cloizeaux (1990) explained that H could be considered equivalent to the number of entanglements per polymer chain. However, the later modeling results demonstrated that M^* should be much larger than molecular weight between entanglements (M_e) (van Ruymbeke et al. 2002a, b; Wasserman and Graessley 1992). The relationship between M^* and M_e is not completely understood, but it is clear that polydispersity adds a complicating factor to this term. This time-dependent relaxation model proposed by des Cloizeaux (1990) simplifies the entangled polymer chain relaxation in terms of a time-dependent stress diffusion point (entanglement point) along the polymer. This approach allows us to only consider the mobility of the entanglement point (polymer–polymer) and attachment point (polymer–filler) without providing complex tube parameters such as correlation length, tube diameter, and tube fluctuation.

Based on this “binary” system theory, the double-reptation model as discussed should be a plausible approach to obtain the polymer dynamic parameters. The following equation is fitted to the data (Sarvestani 2008).

$$G_{\text{reptate}}(t) = G_N^0 \cdot (\phi_s \cdot F_s(t) + \phi_p \cdot F_p(t))^\beta \quad (6)$$

Here, $F(t)$ is the relaxation function of each fraction as presented in Eq. (2), ϕ_s ($\phi_s = 1 - \phi_p$) represents the volume fraction of polymers adsorbed to the fillers, β is an index that depends on the mixing system. In the case of polymer blends without filler, it has been found that mixing rule exponent β around 2.25 provides a better fit than the original value of 2, which could be due to the contributions of higher-order entanglements or could be linked to the tube dilation (Rubinstein and Colby 1988; Rubinstein et al. 1987; van Ruymbeke et al. 2002a, b). In present research, β values are fixed at 2.25 based on theoretical arguments. Notice that both

parts of the polymers have the same molecular weight and chemical structure, so the parameter H is set a constant for both ($H_s = H_p$). Hence, to determine G_N^0 , τ_p , and H , first we fit the $G(t)$ of neat PBS using model with $\phi_s=0$. Once determined from pure polymer data, these parameters are fixed for the composite fits. Through curve fitting, we can get the values of M^* , τ_s , and τ_p . These two reptation times are equal to the lifetime for the entanglement and attachment, respectively. The characteristic time τ_p for “free polymer” fraction is assumed to be attributed to the disentanglement time of a polymer chain in the melt (Sarvestani 2008) and τ_s is the reptation time of adsorbed chains. From these parameters, microscopic dynamics and its effect on the macroscopic enhancements can be deduced.

van Ruymbeke et al. (2002b) noted that reptation models such as Doi–Edwards and time-dependent diffusion–double-reptation (TDD-DR) cannot correctly predict high-frequency response that corresponds to the short-range dynamics, mainly Rouse relaxations rather than reptation. Hence, it is essential to include the Rouse motion in the relaxation function. The full stress relaxation function is then:

$$G(t) = G_{\text{reptate}}(t) + G_{\text{Rouse}}(t) \quad (7)$$

As proposed by Milner and McLeish (1998) and elaborated upon by Pattamaprom et al. (2000) and van Ruymbeke et al. (2002a, b), the Rouse relaxation function of the monodisperse polymer is given by:

$$F_{\text{Rouse}}(t) = \frac{1}{N_e} \left[\sum_{i=N_e}^N \exp\left(\frac{-i^2 t}{\tau_{\text{Rouse}}}\right) + \frac{1}{3} \sum_{i=1}^{N_e} \exp\left(\frac{-i^2 t}{\tau_{\text{Rouse}}}\right) \right] \quad (8)$$

where $N_e = M/M_e$. M_e is the entanglement molecular weight, which can be estimated from $G_N^0 = \rho RT/M_e$. (Ferry 1980). Here, the first term represents fast three-dimensional relaxation of portions of the chain within a single tube segment, and the second term considers the slow longitudinal modes which are confined by the tube to one dimension (hence, factor 1/3). The reptation time τ_{rep} is expected to be larger than the Rouse time τ_{Rouse} by a factor equal to $3Z$ (Z = the number of entanglement segments within the chains) (Rubinstein and Colby 2003). Unlike the double-reptation theory, the contribution of Rouse relaxation to the relaxation modulus $G(t)$ is assumed to obey a linear mixing law as:

$$G_{\text{Rouse}}(t) = G_N^0 \cdot (\phi_s \cdot F_s^{\text{Rouse}}(t) + \phi_p \cdot F_p^{\text{Rouse}}(t)) \quad (9)$$

This equation can be easily added to Eq. (7) to calculate the relaxation modulus $G(t)$ (Pattamaprom et al. 2000; van Ruymbeke et al. 2002a, b). To the best of our knowledge,

because Rouse relaxation should be a highly localized dynamic mode, it is assumed that Rouse relaxation time will not change due to the presence of fillers. So the final fitting equation can be written as:

$$G(t) = G_N^0 \cdot (\phi_s \cdot F_s(t) + \phi_p \cdot F_p(t))^\beta + G_N^0 \cdot F_s^{\text{Rouse}}(t) \quad (10)$$

Characterization of RAF from heat capacity

From the “immobilized layer” theory, the polymer matrix in the nanocomposite consists of three phases: crystalline phase, mobile amorphous fraction (MAF), and rigid amorphous fraction (RAF) (Sargsyan et al. 2007). RAF is an intermediate phase that does not only exist between crystalline and mobile amorphous phases but also as a result of the filler-confined chains. It does not make any contribution to the heat of fusion of the crystalline phase (Chen et al. 2009; Ma et al. 2011; Sargsyan et al. 2007). In present work, we use the temperature-dependent heat capacity curve to calculate the RAF. The heat capacity above T_g can be written as:

$$C_p^{\text{calc}}(T) = \varphi_s C_p^{\text{solid}}(T) + \varphi_{\text{MA}} C_p^{\text{liquid}}(T) \quad (11)$$

$$\varphi_s = \varphi_c + \varphi_{\text{RAF}} \quad (12)$$

where φ_s , φ_c , φ_{RAF} , and φ_{MA} are the solid, crystal, rigid amorphous, and mobile amorphous volume fractions of polymer, respectively. The heat capacities of the solid fraction $C_p^{\text{solid}}(T)$ and liquid fraction $C_p^{\text{liquid}}(T)$ were obtained from linear fitting of the heat capacity curve below T_g and above T_m , respectively. The “end point” of the glassy transition heat capacity step was used to determine the solid fraction φ_s .

Experimental section

Materials

PBS, used in this study, was produced by Showa Highpolymer Co, LTD, with a weight average molecular weight of 90,000 g/mol with PDI 1.6 (determined by GPC). Fumed silica nanoparticles under the trade name AEROSIL 300 were supplied by Evonik, with a surface area of 300 m²/g. Hydrophobic surface modification of fumed silica was carried out using octadecyltrichlorosilane (OTS). OTS was added to toluene at a weight fraction of 5 wt.%. The solution containing fumed silica was stirred for 72 h at room temperature. The solvent was removed by membrane filter and remaining unreacted OTS was removed by washing with methanol. Functionalized silica was dried in a vacuum oven at 373 K for 12 h (Chen et al. 2014).

Nanocomposites preparation

The PBS and fumed silica were vacuum dried at 90 °C for 24 h before extrusion. Master batch composites with 17 wt.% of fumed silica were prepared in a Brabender Plasticorder torque mixer with type 6 sigmoidal rollers at 50 rpm. A Technovel 15-mm Ultrahigh Speed Twin Screw Compounder was used to extrude samples containing 1~5 vol% of fumed silica particles. This co-rotating, intermeshing extruder was set up with a 60:1 L/D with several kneading zones down the length. Melt compounding was performed at screw speeds of 1000 rpm, which is supposed to obtain distributive and dispersive suspension state. The temperature profile from the feed zone to metering zone was set at 120 °C, and the die temperature was 125 °C. The extrudate was cooled by pulling through a water bath. The extruded samples were granulated and vacuum dried at 90 °C for 24 h. Using those pellets a square plaque (10 × 10 × 0.3 cm) was produced by compression molding in a heated hydraulic

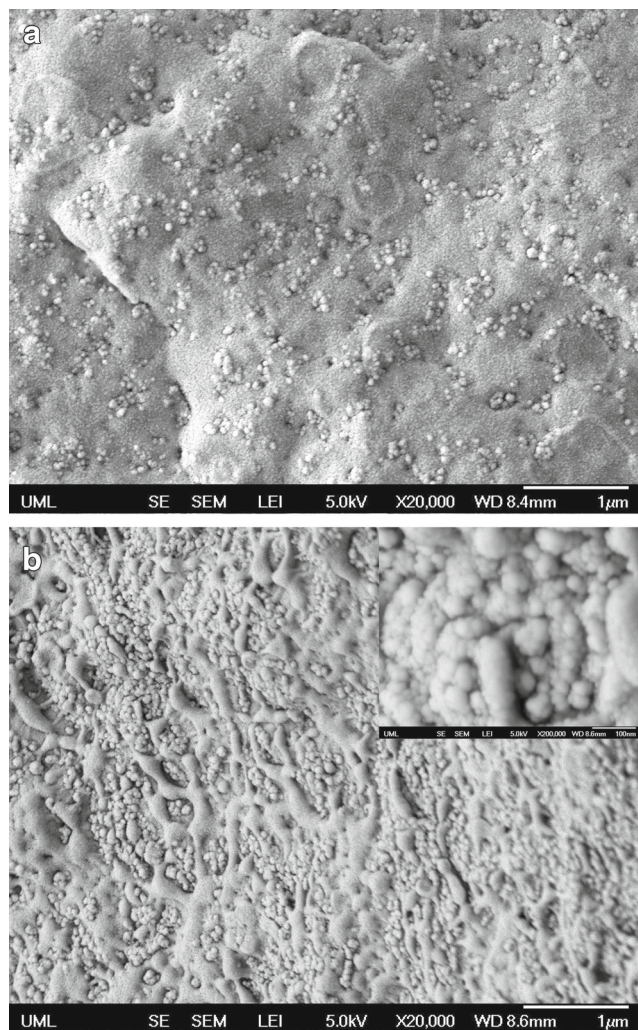


Fig. 1 SEM images of PBS nanocomposites containing **a** 5 vol% AEROSIL and **b** 3.7 vol% OTS-AEROSIL

press (Model: Dake) at 140 °C and 2.5 MPa. Before pressing the pellets, they were held at melt temperature for 10 min to allow degassing and eliminate air bubbles. They were then pressed for another 10 min. After cooling the molded plaque for 10 to 15 min, it was cut into the proper size for rheology test using a band saw.

SEM

The state of dispersion of the fumed silica was observed by field emission scanning electron microscopy (JSM-7401F, Jeol Co., Japan). All specimens were compression molded and cryofractured under liquid nitrogen, and the fracture surfaces were coated with thin layers of gold.

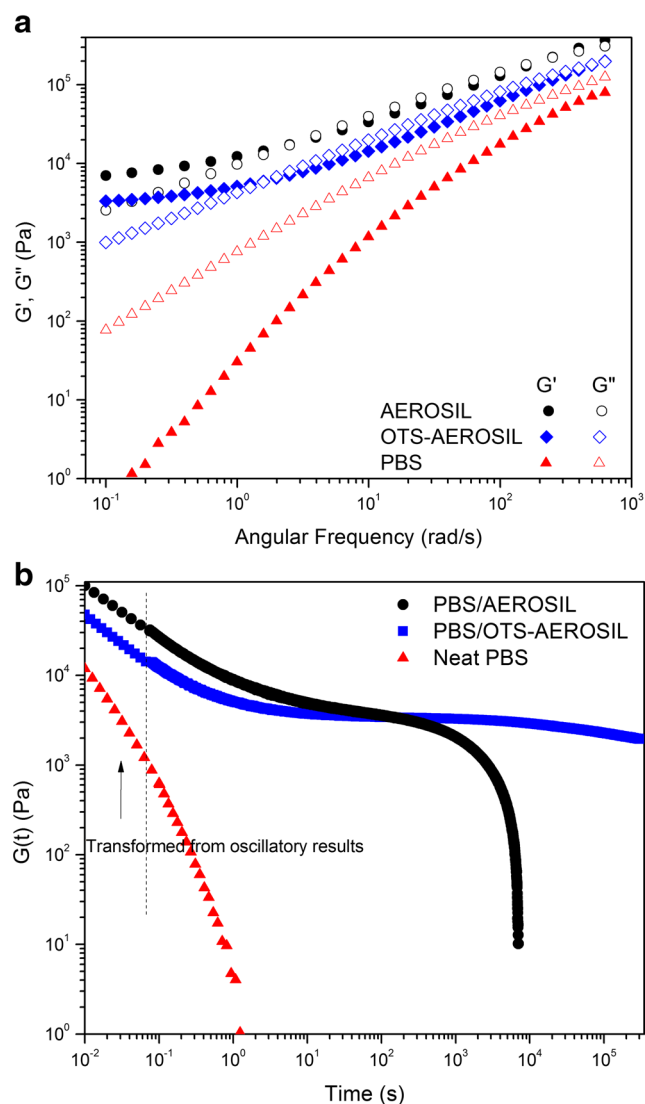


Fig. 2 **a** Dynamic modulus and **b** relaxation modulus of PBS compounding with 3.7 vol% treated and 5 vol% untreated silica fillers at 130 °C

Rheology analysis

The relaxation modulus of PBS/fumed silica nanocomposites was measured by using a parallel-plate rheometer (ARES-G2, TA Instruments) equipped with 25 mm diameter stainless steel parallel disks. Strain sweep measurements were used to determine the linear viscoelastic region. For stress relaxation measurements, the strain amplitude was fixed to 1 % to obtain reasonable signal intensities while remaining in the linear viscoelastic region. Both oscillatory shear and transient shear measurements were performed at 130 °C, which is above the melting temperature ($T_m = 112$ °C). The theoretical model described in above section has been implemented in MatLab in order to obtain parameters in the relaxation function $G(t)$ by curve fitting.

Modulated temperature differential scanning calorimetry

Modulated temperature differential scanning calorimetry (MTDSC) was performed on TA Instruments Discovery DSC instrument in a nitrogen atmosphere. The modulated heating tests were carried out using temperature modulation amplitude of 0.796 K and period, $p = 60$ s. The temperature was increased or decreased with a step of 5 K. To subtract the contribution of silica particles during heating, separate thermal tests on pure silica particles were conducted using the same procedures as for the nanocomposite samples.

Wide angle X-ray diffraction

The X-ray diffraction (XRD) analysis was performed at the ambient temperature on a Scintag XDS-2000 X-ray diffractometer at a scanning rate of 2.0°/min with Cu K α radiation ($\lambda = 0.154$ nm).

Results and discussion

Morphology of PBS/fumed silica nanocomposites

Morphology of the extruded nanocomposites was examined by scanning electron microscopy (SEM), and images are shown in Fig. 1. Several important features should be noted. The PBS nanocomposite containing 3.7 vol% OTS-AEROSIL shows quite different surface texture compared with other samples. The polymer matrix has a rougher texture, and the particle size seems slightly larger. This may indicate that OTS-modified particles interact more intimately with the polymer matrix, causing a coating of the particles rather than debonding at the interface.

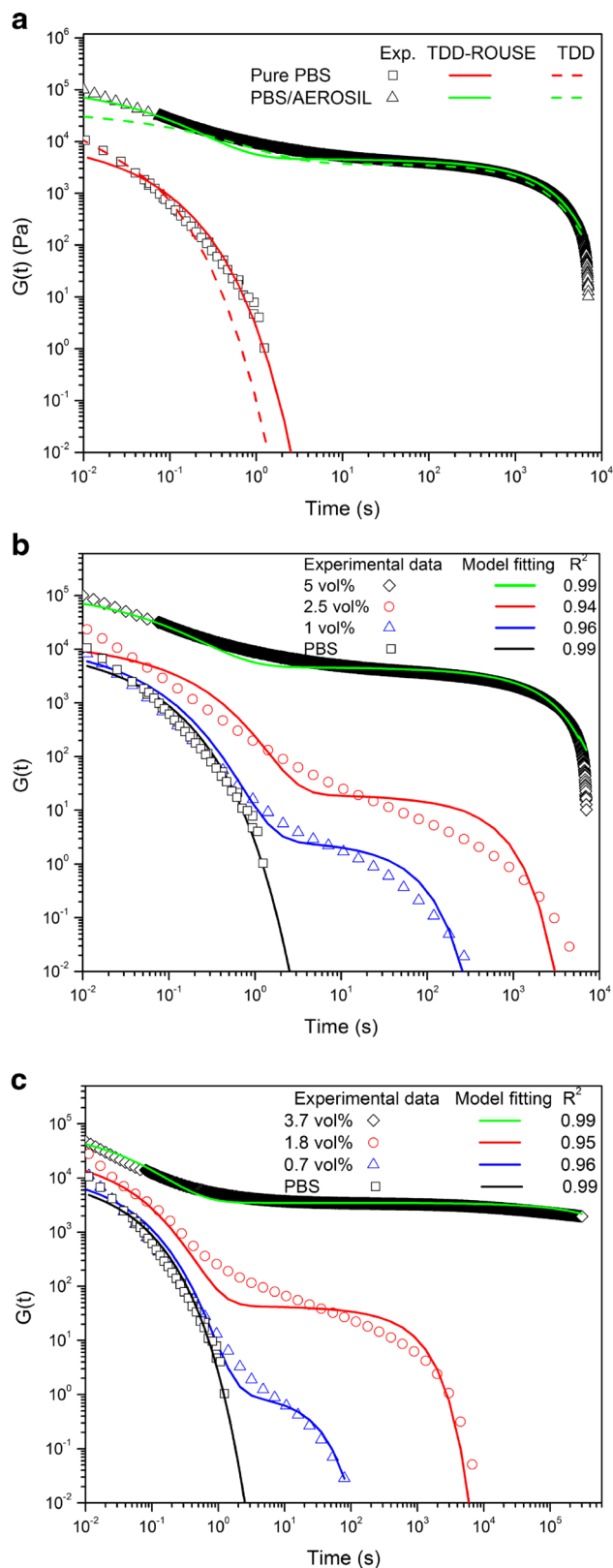


Fig. 3 **a** Fitting relaxation modulus $G(t)$ for 5 vol% AEROSIL/PBS and pure PBS using the TDD-DR with relaxation model (Rouse contribution omitted or included). Experimental and fitting relaxation modulus $G(t)$ using the TDD-DR-Rouse relaxation model for **b** AEROSIL/PBS and **c** OTS-AEROSIL/PBS nanocomposites

Table 1 Parameters for theoretical fit with TDD-DR and TDD-DR-Rouse model to experimental data of 5 vol% AEROSIL/PBS and 3.7 vol% OTS-AEROSIL/PBS nanocomposites

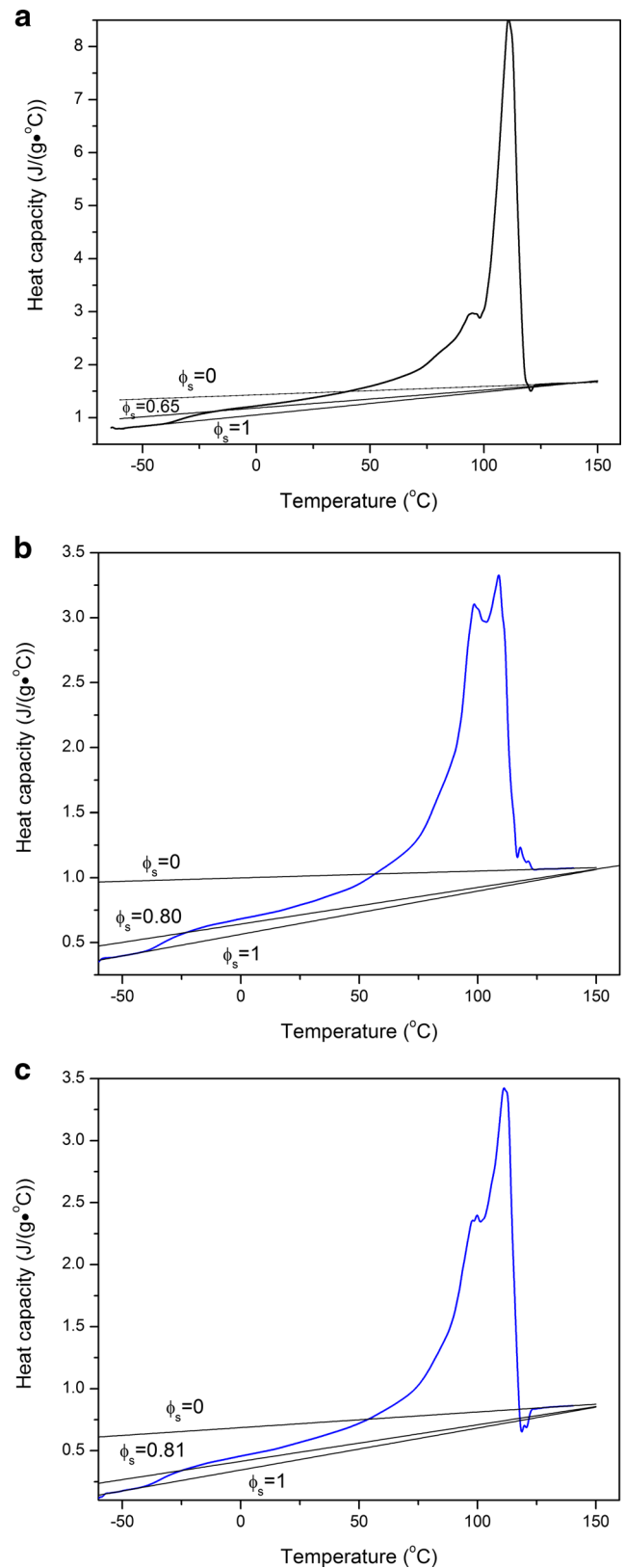
Sample ID	Model	τ_s^{Rep} (s)	β	ϕ_s
AEROSIL-5	TDD-DR-Rouse	7900	2.25	0.20
	TDD-DR	8910	4.7	0.40
OTS-AEROSIL-3.7	TDD-DR-Rouse	4.4×10^6	2.25	0.24
	TDD-DR	6.2×10^6	5.3	0.45

Viscoelastic analysis

Figure 2 shows that PBS/fumed silica nanocomposites with high filler concentration usually display solid-like or highly entangled rheological behavior at the low frequencies, indicating the presence of network structures. The elastic responses on longer time scales of such networks were investigated by using transient rheology test. To extend the scale to the short time range, oscillatory shear modulus curves were transformed to the relaxation modulus curves by means of calculating relaxation spectrum (Chen et al. 2014). As shown in Fig. 2b, both the PBS/unmodified fumed silica nanocomposites display typical polymer melt viscoelastic properties at long relaxation times, which is characteristic of entanglement for a temporary physical network. Compared with neat PBS, the nanocomposites display significantly higher modulus and longer relaxation time. The PBS/OTS-modified AEROSIL nanocomposites show a similar plateau modulus but longer relaxation time than for pure AEROSIL with the same screw speed. This extended rubbery-like behavior is consistent to our previous study on the samples manufactured by low-shear mixing approach (Chen et al. 2014). This may also correspond to the special texture that we observed from SEM images. Therefore, the surface treatment can increase either the amount or the strength of temporary crosslinking of PBS molecules and further cause rubbery-like behavior. Surface compatibilization also results in an increase in the time that samples need to fully relax, although the initial modulus is lower than for the untreated filler.

Table 2 Parameters for theoretical fit with TDD-DR-Rouse model to experimental data of polymer nanocomposites

Sample ID	τ_s^{Rep} (s)	β	ϕ_s
AEROSIL-1	165	2.25	0.012
AEROSIL-2.5	1810	2.25	0.035
AEROSIL-5	7900	2.25	0.20
OTS-AEROSIL-0.7	76	2.25	0.0083
OTS-AEROSIL-1.8	3163	2.25	0.035
OTS-AEROSIL-3.7	4.4×10^6	2.25	0.24

**Fig. 4** Specific reversing heat capacity from TMDSC for **a** PBS, **b** 5 vol% AEROSIL/PBS, and **c** 3.7 vol% OTS-AEROSIL/PBS nanocomposites during modulated reheating

Relaxation of PBS chains with TDD-DR-Rouse model

To determine the amount of confined polymer layer, we fit the relaxation modulus using Eq. (10). The fractions and characteristic times are extracted from the fit. The experimental value of plateau modulus G_N^0 , Rouse time τ_p^{Rouse} , reptation time τ_p^{Rep} , and H are 2.85×10^5 Pa, 1.79 s, 0.03 s, and 0.12, respectively. Kabanemi and Héту (2013) demonstrated that filler loadings will not affect the G_N^0 , so we fix this value as constant in further fittings. Using $G_N^0 = \rho RT/M_e$ a molecular weight between entanglements M_e of 11,000 g/mol at 130 °C ($\rho = 1.23$ g/cm³) is obtained. This value is slightly larger than M_e mentioned in the papers for other aliphatic polyesters such as PLA (~9000 g/mol) (Dorgan et al. 1999). According to Yokohara and Yamaguchi (2008), it was expected that M_e of PLA is lower than that of PBS. The results obtained with the TDD-DR-Rouse model are shown in Fig. 3.

It is clear from Fig. 3a that we obtain a good agreement between experimental results and the model fits by either TDD-DR model or including the Rouse contribution in the TDD-DR model; however, visual inspection shows that each model fits better over different time ranges. To evaluate the applicability of each model, Table 1 compares the parameters extracted from the TDD-DR with and without Rouse contribution. We have found much better agreement by consistently taking β around 5 for the TDD-DR model. According to double-reptation theory, the value of β should be between 2 and 2.3 (des Cloizeaux 1988; Dealy and Larson 2006; Tsenoglou 1987). To fit the high dynamics Rouse regime with the double-reptation model, Maier et al. (1998) reported some polymers with higher β values: $\beta = 3.84$ for PS and $\beta = 3.3$ for PMMA. However, there is no physical basis for this high mixing index from double-reptation theory. Therefore, inclusion of the Rouse contribution in the TDD-DR provides a more correct physical representation of the system.

As shown in Fig. 3b, c, the model fits the experimental data of PBS nanocomposites with high fumed silica concentration well at both short and long times. It should be noted, however, that the model fails to fit to the experimental data at intermediate times for low filler concentration. One possible reason for the poor fit is the smearing of the relaxation spectrum that can be expected due to polydispersity. Another possibility is the existence of relaxation or diffusion mechanisms other than

reptation not taken into account by the model, such as chain length fluctuation resulting from the free ends of attached chains (Kabanemi and Héту 2010). This relaxation mechanism usually plays important role in intermediate time range (Milner and McLeish 1998). For low filler loadings, the free ends fluctuation and reptation contributions to $G(t)$ may occur over similar time ranges. The fluctuation term in Eq. (3) may not be able to cover the mobility of such star-shaped segments (Kabanemi and Héту 2010; Pearson and Helfand 1984). Repeating the measurements with monodisperse samples and for differing molecular weights could disambiguate the source of this error. Table 2 summarizes the values of the parameters extracted from fitting. It appears that that the particle surface adsorbs and confines a larger fraction of the polymer chains after hydrophobic surface treatment. According to the definition of reptation time, the higher relaxation time for the same polymer chains is due to the increase in friction coefficient ζ and the entanglement density determined by the polymer–particle interactions. It is also clear from Table 2 that the ϕ_s is not directly proportional to the filler volume fraction for either filler type. The nonlinear relationships found between ϕ_s and filler concentration are challenging to explain, since we do not have the quantitative dispersion information for the fillers. We speculate that the disproportionate surface area to volume ratio could be caused by differences in particle aggregation or a thicker bound layer with higher filler fractions (Ma et al. 2011). To verify the uniqueness of the fitting results, sensitivity analysis has been done as shown in support materials.

Thermal analysis

This study also aims to establish a plausible correlation between confined polymer fraction between rheology and thermal analysis based on the RAF theory (Chen et al. 2009; Ma et al. 2011; Sargsyan et al. 2007). The solid fraction φ_s was determined by using Eq. (11) to simulate a line which passes through the end point of the glass transition. Because only the crystals and RAF remain in the solid state, the RAF can be calculated from Eq. (12), where the degree of crystallinity of the polymer matrix was determined from X-ray diffraction of annealed samples (data not shown).

Table 3 Thermal properties of the PBS matrix in PBS/fumed silica nanocomposites

Sample ID	φ_c (± 0.01)	φ_s (± 0.01)	φ_{ra} (± 0.02)	φ_{ra}' (± 0.02)	Fraction-confined polymer ϕ_s (from rheology model)
PBS	0.49	0.64	0.15	0	
AEROSIL-5	0.40	0.80	0.40	0.25	0.20
OTS-AEROSIL-3.7	0.38	0.81	0.43	0.28	0.24

From the TMDSC results shown in Fig. 4, the solid fraction of polymer matrix increased with 10 % silica loading of either surface treatment, which means the “mobile” amorphous fraction decreased. This is probably due to a decrease in the free volume of the polymer chains and further restriction of molecular mobility near the interface. Based on φ_s , φ_c , and Eq. (12), we obtain the RAF for those samples as listed in Table 3.

With the addition of fumed silica a large increase in RAF was observed. The value of φ_{ra} reaches 0.43 for the OTS-treated fumed silica. This value includes the contributions of the rigid amorphous interphase between crystalline and mobile amorphous phases. To estimate the amount of immobilized polymer, the φ_{ra} values for nanocomposites were corrected by subtracting the contribution of pure polymer. The corrected RAF φ_{ra}' values are also shown in Table 3. It can be found from Table 3 that the OTS-functionalized silica results in a significantly higher RAF (note the lower particle volume fraction). More interestingly, the values of φ_{ra}' are comparable with the fraction of confined polymer ϕ_s obtained from the rheology model. Note that this “immobilized layer” is a temperature-dependent concept used to describe the solid-state phase; it has been demonstrated by Arrighi that the fraction of immobilized chains decreases with increased temperature (Arrighi et al. 1998). It is clear from the rheology results, however, that the confined polymer dynamics do not disappear in the liquid state. Interestingly, the same fraction of strongly immobilized polymer found in the solid state (φ_{ra}') still presents restricted dynamics in the melt state. The good quantitative agreement between the rheology model results and thermal analysis may have important implications for the processing and performance tradeoffs in nanocomposite engineering.

Conclusions

Dynamic relaxation characteristics determining the molecular structure of fumed silica-filled PBS composites have been explored in the present work. We have shown that the TDD-DR model that takes into account Rouse relaxation can be used to predict the molecular structure and determine the strength of interactions in polymer nanocomposites from their linear viscoelastic response. The results obtained are in quantitative agreement with the values estimated from the changes in the heat capacity step in the glass transition region. Control of surface functionality yields higher strength PBS composites due to strong polymer–filler interactions and large fraction of bound polymer layer. This is likely to enhance the toughness of these composites as well since

multiple mechanisms are available for adsorbing energy over a wide range of shear rates.

Acknowledgments This research was funded through support from NSF EEC-1342229.

References

- Akcora P, Kumar SK, Garcia Sakai V, Li Y, Benicewicz BC, Schadler LS (2010) Segmental dynamics in PMMA-grafted nanoparticle composites. *Macromolecules* 43:8275–8281. doi:10.1021/ma101240j
- Akcora P, Kumar SK, Moll J, Lewis S, Schadler LS, Li Y, Benicewicz BC, Sandy A, Narayanan S, Ilavsky J, Thiyagarajan P, Colby RH, Douglas JF (2009a) “Gel-like” mechanical reinforcement in polymer nanocomposite melts. *Macromolecules* 43:1003–1010. doi:10.1021/ma902072d
- Akcora P, Liu H, Kumar SK, Moll J, Li Y, Benicewicz BC, Schadler LS, Acehan D, Panagiotopoulos AZ, Pryamitsyn V, Ganesan V, Ilavsky J, Thiyagarajan P, Colby RH, Douglas JF (2009b) Anisotropic self-assembly of spherical polymer-grafted nanoparticles. *Nature Materials* 8:354–359. http://www.nature.com/nmat/journal/v8/n4/supinfo/nmat2404_S1.html
- Anderson BJ, Zukoski CF (2009) Rheology and microstructure of entangled polymer nanocomposite melts. *Macromolecules* 42:8370–8384. doi:10.1021/ma9011158
- Aranguren MI, Mora E, DeGroot JV, Macosko CW (1992) Effect of reinforcing fillers on the rheology of polymer melts. *J Rheol* 36:1165–1182. doi:10.1122/1
- Arrighi V, Higgins JS, Burgess AN, Floudas G (1998) Local dynamics of poly(dimethyl siloxane) in the presence of reinforcing filler particles. *Polymer* 39:6369–6376. http://dx.doi.org/10.1016/S0032-3861(98)00139-6
- Chen H, Liu Z, Cebe P (2009) Chain confinement in electrospun nanofibers of PET with carbon nanotubes. *Polymer* 50:872–880. doi:10.1016/j.polymer.2008.12.030
- Chen X, Gug J, Sobkowicz MJ (2014) Role of polymer/filler interactions in the linear viscoelasticity of poly(butylene succinate)/fumed silica nanocomposite. *Composites Science and Technology* 95:8–15. http://dx.doi.org/10.1016/j.compscitech.2014.01.025
- Chou TW (1993) Structure and properties of composites. VCH
- des Cloizeaux J (1988) Double reptation vs. simple reptation in polymer melts. *Europhys Lett* 5:437–442
- des Cloizeaux J (1990) Relaxation and viscosity anomaly of melts made of long entangled polymers time-dependent reptation. *Macromolecules* 23:4618–4687
- de Gennes PG (1971) Reptation of a polymer chain in the presence of fixed obstacles. *The Journal of Chemical Physics* 55:572. doi:10.1063/1.1675789
- Dealy JM, Larson RG (2006) Structure and rheology of molten polymers. Hanser Publications, Munich
- Dionne PJ, Ozisik R, Picu CR (2005) Structure and dynamics of polyethylene nanocomposites. *Macromolecules* 38:9351–9358
- Doi M, Edwards SF (1978) Dynamics of concentrated polymer systems. Part 2.—molecular motion under flow. *Journal of the Chemical Society, Faraday Transactions 2: Molecular and Chemical Physics* 74:1802–1817
- Doi M, Edwards SF (1986) The theory of polymer dynamics. Clarendon Press, Oxford
- Dorgan JR, Williams JS, Lewis DN (1999) Melt rheology of poly(lactic acid): Entanglement and chain architecture effects. *Journal of Rheology* (1978–present) 43:1141–1155. doi:http://dx.doi.org/10.1122/1.551041

- Drozdov AD, Høg Lejre AL, Jd C (2009) Viscoelasticity, viscoplasticity, and creep failure of polypropylene/clay nanocomposites. *Compos Sci Technol* 69:2596–2603. doi:10.1016/j.compscitech.2009.07.018
- Ferry JD (1980) *Viscoelastic properties of polymers*. Wiley
- Gagliardi S, Arrighi V, Ferguson R, Telling MTF (2001) Restricted dynamics in polymer-filler systems. *Physica B: Condensed Matter* 301:110–114 [http://dx.doi.org/10.1016/S0921-4526\(01\)00520-8](http://dx.doi.org/10.1016/S0921-4526(01)00520-8)
- Harton SE, Kumar SK, Yang H, Koga T, Hicks K, Lee H, Mijovic J, Liu M, Vallery RS, Gidley DW (2010) Immobilized polymer layers on spherical nanoparticles. *Macromolecules* 43:3415–3421. doi:10.1021/ma902484d
- Havet G, Isayev AI (2001) A thermodynamic approach to the rheology of highly interactive filler-polymer mixtures: part I—theory. *Rheol Acta* 40:570–581. doi:10.1007/s003970100176
- Havet G, Isayev AI (2003) A thermodynamic approach to the rheology of highly interactive filler-polymer mixtures. Part II. Comparison with polystyrene/nanosilica mixtures. *Rheol Acta* 42:47–55. doi:10.1007/s00397-002-0253-z
- Jouault N, Vallat P, Dalmas F, Sr S, Jestin J, Fo B (2009) Well-dispersed fractal aggregates as filler in polymer–silica nanocomposites long-range effects in rheology. *Macromolecules* 42:2031–2040
- Kabanemi KK, Héту J-F (2010) A reptation-based model to the dynamics and rheology of linear entangled polymers reinforced with nanoscale rigid particles. *J Non-Newtonian Fluid Mech* 165:866–878. doi:10.1016/j.jnnfm.2010.04.006
- Kabanemi KK, Héту J-F (2013) Reptation model for the dynamics and rheology of particle reinforced polymer chains. In: Mittal V (ed) *Modeling and prediction of polymer nanocomposite properties*, vol 4. Wiley-VCH
- Kirst KU, Kremer F, Litvinov VM (1993) Broad-band dielectric spectroscopy on the molecular dynamics of bulk and adsorbed poly(dimethylsiloxane). *Macromolecules* 26:975–980. doi:10.1021/ma00057a015
- Leblanc JL (2009) *Filled polymers: science and industrial applications*. Taylor & Francis
- Litvinov VM, Spiess HW (1991) 2 H NMR study of molecular motions in polydimethylsiloxane and its mixtures with aerosils. *Die Makromolekulare Chemie* 192:3005–3019. doi:10.1002/macp.1991.021921216
- Litvinov VM, Zhdanov AA (1987) Molecular motions in filled polydimethylsiloxanes. *Polymer Science USSR* 29:1133–1140 DOI [http://dx.doi.org/10.1016/0032-3950\(87\)90127-4](http://dx.doi.org/10.1016/0032-3950(87)90127-4)
- Liu M, Pu M, Ma H (2012) Preparation, structure and thermal properties of polylactide/sepiolite nanocomposites with and without organic modifiers. *Compos Sci Technol* 72:1508–1514. doi:10.1016/j.compscitech.2012.05.017
- Long D, Sotta P (2007) Stress relaxation of large amplitudes and long timescales in soft thermoplastic and filled elastomers. *Rheol Acta* 46:1029–1044. doi:10.1007/s00397-007-0187-6
- Ma Q, Mao B, Cebe P (2011) Chain confinement in electrospun nanocomposites: using thermal analysis to investigate polymer–filler interactions. *Polymer* 52:3190–3200. doi:10.1016/j.polymer.2011.05.015
- Maier D, Eckstein A, Friedrich C, Honerkamp J (1998) Evaluation of models combining rheological data with the molecular weight distribution. *Journal of Rheology* (1978–present) 42:1153–1173 doi: <http://dx.doi.org/10.1122/1.550952>
- Milner ST, McLeish TCB (1998) Reptation and contour-length fluctuations in melts of linear polymers. *Phys Rev Lett* 81:725–728
- Moll JF, Akcora P, Rungta A, Gong S, Colby RH, Benicewicz BC, Kumar SK (2011) Mechanical reinforcement in polymer melts filled with polymer grafted nanoparticles. *Macromolecules* 44:7473–7477. doi:10.1021/ma201200m
- Mortezaei M, Famili MHN, Kokabi M (2011) The role of interfacial interactions on the glass-transition and viscoelastic properties of silica/polystyrene nanocomposite. *Compos Sci Technol* 71:1039–1045. doi:10.1016/j.compscitech.2011.02.012
- Najafi N, Heuzey MC, Carreau PJ (2012) Polylactide (PLA)-clay nanocomposites prepared by melt compounding in the presence of a chain extender. *Compos Sci Technol* 72:608–615. doi:10.1016/j.compscitech.2012.01.005
- Oh H, Green PF (2008) Polymer chain dynamics and glass transition in athermal polymer-nanoparticle mixtures. *Nat Mater* 8:139–143. doi:10.1038/nmat2354
- Pattamaprom C, Larson RG, Van Dyke TJ (2000) Quantitative predictions of linear viscoelastic rheological properties of entangled polymers. *Rheol Acta* 39:517–531. doi:10.1007/s003970000104
- Pearson DS, Helfand E (1984) Viscoelastic properties of star-shaped polymers. *Macromolecules* 17:888–895. doi:10.1021/ma00134a060
- Rubinstein M, Colby RH (1988) Self-consistent theory of polydisperse entangled polymers: linear viscoelasticity of binary blends. *The Journal of Chemical Physics* 89:5291. doi:10.1063/1.455620
- Rubinstein M, Colby RH (2003) *Polymer physics*. Oxford University Press, New York
- Rubinstein M, Helfand E, Pearson DS (1987) Theory of polydispersity effects on polymer rheology. Binary distribution of molecular weights. *Macromolecules* 20:822–829
- van Ruymbeke E, Keunings R, Bailly C (2002a) Determination of the molecular weight distribution of entangled linear polymers from linear viscoelasticity data. *J Non-Newtonian Fluid Mech* 105:153–175
- van Ruymbeke E, Keunings R, Stéphenne V, Hagenaaers A, Bailly C (2002b) Evaluation of reptation models for predicting the linear viscoelastic properties of entangled linear polymers. *Macromolecules* 35:2689–2699
- Sargsyan A, Tonoyan A, Davtyan S, Schick C (2007) The amount of immobilized polymer in PMMA SiO₂ nanocomposites determined from calorimetric data. *European Polymer Journal* 43:3113–3127 <http://dx.doi.org/10.1016/j.eurpolymj.2007.05.011>
- Sarvestani AS (2008) Modeling the solid-like behavior of entangled polymer nanocomposites at low frequency regimes. *Eur Polym J* 44: 263–269. doi:10.1016/j.eurpolymj.2007.11.023
- Sarvestani AS, Jabbari E (2006) Modeling and experimental investigation of rheological properties of injectable poly(lactide ethylene oxide fumarate)/hydroxyapatite nanocomposites. *Biomacromolecules* 7: 1573–1580
- Sarvestani AS, Jabbari E (2008) A model for the viscoelastic behavior of nanofilled hydrogel composites under oscillatory shear loading. *Polym Compos* 29:326–336. doi:10.1002/pc.20416
- Sarvestani AS, Picu CR (2004) Network model for the viscoelastic behavior of polymer nanocomposites. *Polymer* 45:7779–7790. doi:10.1016/j.polymer.2004.08.060
- Sarvestani AS, Picu CR (2005) A frictional molecular model for the viscoelasticity of entangled polymer nanocomposites. *Rheol Acta* 45:132–141. doi:10.1007/s00397-005-0002-1
- Shenoy AV (1999) *Rheology of filled polymer systems*. Springer
- Simhambhatla M, Leonov AI (1995) On the rheological modeling of filled polymers with particle-matrix interactions. *Rheol Acta* 34: 329–338. doi:10.1007/BF00367150
- Sternstein SS, Zhu A-J (2002) Reinforcement mechanism of nanofilled polymer melts as elucidated. *Macromolecules* 35:7262–7273
- Subbotin A, Semenov A, Doi M (1997) Friction in strongly confined polymer melts: effect of polymer bridges. *Phys Rev E* 56:623–630
- Tsagaropoulos G, Eisenberg A (1995) Dynamic mechanical study of the factors affecting the two glass transition behavior of filled polymers. Similarities and Differences with Random Ionomers. *Macromolecules* 28:6067–6077. doi:10.1021/ma00122a011

- Tsenoglou C (1987) Viscoelasticity of binary homopolymer blends. *Polym Prepr Am Chem Soc Div Polym Chem* 28:185–186
- Tsenoglou C (1991) Molecular weight polydispersity effects on the viscoelasticity of entangled linear polymers. *Macromolecules* 24:1762–1767
- Wasserman SH, Graessley WW (1992) Effects of polydispersity on linear viscoelasticity in entangled polymer melts. *Journal of Rheology* (1978-present) 36:543–572 doi:<http://dx.doi.org/10.1122/1.550363>
- Yokohara T, Yamaguchi M (2008) Structure and properties for biomass-based polyester blends of PLA and PBS. *European Polymer Journal* 44:677–685 <http://dx.doi.org/10.1016/j.eurpolymj.2008.01.008>
- Zhang Q, Archer LA (2002) Poly(ethylene oxide)-silica nanocomposites structure and rheology. *Langmuir* 18:10435–10442
- Zhu A-J, Sternstein SS (2003) Nonlinear viscoelasticity of nanofilled polymers: interfaces, chain statistics and properties recovery kinetics. *Composites Science and Technology* 63:1113–1126 [http://dx.doi.org/10.1016/S0266-3538\(03\)00032-0](http://dx.doi.org/10.1016/S0266-3538(03)00032-0)
- Zhu Z, Thompson T, Wang S-Q, von Meerwall ED, Halasa A (2005) Investigating linear and nonlinear viscoelastic behavior using model silica-particle-filled polybutadiene. *Macromolecules* 38:8816–8824. doi:[10.1021/ma050922s](https://doi.org/10.1021/ma050922s)